Desalination and Water Treatment
www.deswater.com

doi:10.5004/dwt.2019.23913

153 (2019) 321–337
June

Adsorption of Acid Blue 113 from aqueous solution onto nutraceutical industrial coriander seed spent: Isotherm, kinetics, thermodynamics and modeling studies

Syed Noeman Taqui[a], Rosiyah Yahya[a,*], Aziz Hassan[a], Nayan Nayak[b], Akheel Ahmed Syed[c]

[a]*Department of Chemistry, University of Malaya, Kuala Lumpur-50603, Malaysia, email: noemansyed89@gmail.com (S.N. Taqui), Tel. +60-192683006, email: rosiyah@um.edu.my (R. Yahya), ahassan@um.edu.my (A. Hassan),*
[b]*LAQV-REQUIMTE, Department of Chemistry, Faculty of Science and Technology, Universidade NOVA de Lisboa, Caparica, Portugal, email: nayaknayan@gmail.com (N. Nayak)*
[c]*Department of Studies in Chemistry, University of Mysore, Manasa Gangotri, Mysuru - 570006, India, email: akheelahmed54@gmail.com (A.A. Syed)*

Received 4 August 2018; Accepted 2 February 2019

ABSTRACT

In this study, use of low-cost nutraceutical industrial coriander seed spent (NICSS) for removing Acid Blue 113 (AB113) from aqueous solution has been explored. Biosorption studies were done under varying conditions of initial pH, initial dye concentration, adsorbent dosage, particle size of the adsorbent and temperature to assess the adsorption capacity, kinetics and equilibrium thermodynamics. Optimal adsorption took place at acidic pH. A two-level fractional factorial experimental design (FFED) and analysis of variance (ANOVA) showed that a maximum adsorption value of 90.00 mg/mL was possible. The influence of each parameter and combination of parameters on the final adsorption capacity of the system was studied. The dye uptake followed a pseudo-second order kinetic paradigm and was best described by the Langmuir isotherm. Intra-particle diffusion showed that the adsorption mechanism was more governed by external mass transfer. AB113 adsorption on NICSS was endothermic and almost spontaneous. The NICSS has a highly fibrous matrix with hierarchical porous structure as evidenced by SEM images. Analysis of the spent showed that it possesses cellulosic and ligno-cellulosic materials having both hydrophilic and hydrophobic properties. The results proved that NICSS efficiently removes AB113 from water and textile industrial effluents.

Keywords: Acid Blue 113; Nutraceutical industrial coriander seed spent; Adsorption studies; Isotherms; Kinetics; Modeling

1. Introduction

The ever-increasing volume of waste from textile industry is posing serious environmental problems in majority of Asian countries. The inevitability of development of a holistic system to deal with it has become an indispensable socio-economic and environmental issue for the sustainable development of world textile industry which produces about 60 billion kg of fabric and consuming over nine trillion gallons of water [1]. Textile industry is one amongst the top ten polluting industries which use a variety of synthetic dyes adding 200,000 tons of dyes every year to the industrial effluents [2]. These dyes are visible even in amounts of <1 mg/L in water. This situation seriously creates problems with respect to quality and transparency of water in lakes and rivers, affecting the aquatic environment [3].

Azo dyes possessing nitrogen double bond, (–N=N–) constitute nearly 70% of commercial synthetic dyes produced and used by textile industry [4,5]. The predominance of azo dyes is due to their ease and cost effectiveness for synthesis, great structural diversity, high molar extinction coefficient, and medium-to-high fastness properties [6]. The textile industries face the problems of removal of the dye colors as they are resistant to biodegradation and possess carcinogenic and mutagenic properties [7].

*Corresponding author.

The Acid Blue 113 (AB113) dye categorized as benzidine-based bisazo anionic dye is extensively used in textile industries to dye wool, silk and polyamide fibres [8]. It may ultimately get metabolized to benzidine, a known human carcinogen [9]. The health problems caused by AB113 will increase, with growing use by textile industry. Hence, it is imperative to abate the AB113 footprint in the environment resulting from textile effluents. So far only limited reports are published on decolouration, degradation and/or adsorption of AB113 from water. The techniques, methods and procedures reported could be categorized into; biological-cum-chemical, electro-coagulation, physical methods using UV radiations, photo-catalytic degradation, low frequency ultrasound assisted degradation, nanomaterials, and use of inorganic materials including activated carbons. High cost of plant establishment, increased operation cost, problem of regeneration, secondary pollutants, sensitivity to changes in wastewater input, interference by wastewater ingredients, and disposal of residual sludge are some associated technological and economical drawbacks of above methods [10,11]. Limited literature is available on the use of low-cost agro-industrial waste for the remediation of AB113 in aqueous solution [12].

Adsorption as a technique for removing toxic dyes from aqueous solutions is i) simple in operation, ii) high treatment efficiency without discharging any harmful by-products to treated water and iii) easy scaling up from laboratory to field level [13]. Uses of activated carbon and nanomaterials as adsorbents have been investigated for the removal of AB113 from water. Ideal biosorbent for remediation of dyes should be available in abundance at low price; have no or minimal other use(s) to control price rise and stabilize in demand; be available in ready-to-use form without requiring any pre-chemical treatment; have such pore structure as to permit better adsorption; be adoptable to simple and cost-effective technology to reuse the sludge/toxic biomass produced after the remediation process.

The use of nutraceutical industrial coriander seed spent (NICSS) for the bioremediation of AB113 from water possesses economic, society and environmental sustainability. Coriander seeds come under Nutraceuticals category. The rising demand for nutraceuticals across the world as alternative to allopathy or modern systems of medicine has attracted the attention of many industries especially pharmaceutical companies. Transparency Market Research, has fore casted that the global nutraceuticals market is expanding at a CAGR of 7.3% from 2015 to 2021 which was valued at US$ 182.6 bn in 2015, is going to reach US$278.95 bn by the end of 2021 [14]. Though there are no reports mentioning about the spent/waste generated in nutraceutical industrial sector, but, looking at the volume of the market turn-over the spent/waste generated may run in to millions of tons.

Coriander (*Coriandrum sativum L.*) is *Apiceae* family and genus *Coriandrum L*. India is the highest producer, as also the consumer and exporter of this spice with greater share in world export market with annual production of 3.15×10^5 tons [15]. Extraction of oleoresin from coriander involves mechanical, chemical and thermal processes. The resultant spent obtained is known as nutraceutical industrial coriander seed spent (NICSS) and is a ready-to-use good biosorbent with minimum E-factor [16]. Moreover, myriad research papers published on adsorptive remediation of dyes from aqueous water and/or industrial effluents, have limited published information available regarding the disposal of the dye adsorbed biosorbent or otherwise known as "sludge". Our research school is the first to report the use of Nutraceutical Industrial Spent (NIS) and the dye adsorbed as filler/reinforcing material(s) for the fabrication of composites [17–25] and as effective adsorbents for remediation of Congo red, methylene blue and ethidium bromide dyes [26–28].

In the present work, we have attempted to show the effectiveness of coriander seed spent, an agro-industry byproduct, in adsorbing AB113 from water. We have attempted further, to understand the mechanism of adsorption by fitting the data to available isotherm models. We have also attempted to understand the chemical stability and feasibility of the process by determining the thermodynamic parameters. Subsequently, to understand the factors affecting the adsorption we have modeled the kinetics of the process at different temperatures. Using this data we have designed a fractional factorial experimental design to statistically optimize, making it suitable for scaling up the whole process. This adsorbed AB113-coriander seed spent material could be further used as fillers in thermo composites to be used as low-cost building materials completely mitigating the footprint of AB113 from the environment.

2. Experimental

2.1. Materials

The dye used for this experiment is acid blue 113 (AB113) also commonly referred to as Neutral Blue 5R; [C.I. = 26360; CAS Number: 3351-05-1; chemical formula = $C_{32}H_{21}N_5Na_2O_6S_2$; molecular weight = 681.65; absorbance maximum (λ_{max}) = 566 nm]. The molecular structure of the dye is shown in Fig. 1.

2.2. Adsorbent preparation and characterization

2.2.1. Adsorbent preparation

NICSS was obtained from a local factory (Fig. 2) in order to be as close to real world application as possible. The NICSS was first dried in sunlight, then crushed and finally ground using a ball mill and sieved as per ASTM standard particle size: ≥ 125 μm ≤ 177 μm (ASTM 80 mesh particles).

2.2.2. Surface characterization

Scanning electron microscope (SEM, LEO 435 VP model, Japan) was used to visualize the surface morphology of the

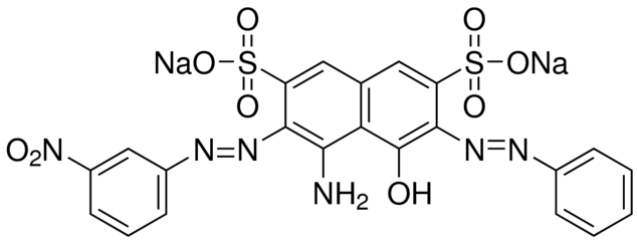

Fig. 1. Structure of Acid Blue 113 dye.

Fig. 2. Coriander seeds, coriander seed spent and coriander seed spent powder.

NICSS and AB113-loaded samples. Fourier transform infrared spectrometry (FTIR, Inter-spec 2020, Spectro Lab, UK) was used to determine the functional groups on the sample surface.

The surface charge of NICSS was determined by preparing stock solution of 0.1 M KCl. Fifty ml each of 0.1 M KCl were transferred to seven 250-ml Erlenmeyer flasks and pH was adjusted initially to 2.0 and 12.0 by using HCl and NaOH. NICSS (0.05 g) was added to each flask. After allowing for 24 h the final pH was measured by pH meter (Systronics-802, India). Graph of pH_{final} *vs.* $pH_{initial}$ was plotted [29].

Measurement of specific surface area a_{sBET} was done by N_2 adsorption at 77 kelvin using a BELSORP, Japan surface area analyzer and the value was determined at 1.186 $m^2\ g^{-1}$.

2.3. Batch adsorption experiments

The experiments were conducted in batches with varying parameters. However, the common preliminary preparation involved the setting up of 250-mL flasks with 50 mL working aqueous solution of AB113 (100 mg/L). After the initial preparation was complete, 50 mg of NICSS was introduced into each flask. A temperature-controlled shaker was used to agitate the contents of the flasks at 165 rpm for 3 h. Evaluations were then conducted based on the effects of varying parameters such as, dosage of NICSS (0.025, 0.050, 0.075, 0.100, 0.150, 0.200, 0.300 g/50 ml); AB113 concentration (25, 50, 75, 100, 125, 150, 175, 200, 300, 400 and 500 mg/L); pH (2, 4, 6, 7, 8, 10 and 12) and temperature (303 K, 313 K and 323 K) with different dye concentration (100, 150, 200 ppm). The samples were centrifuged for five minutes to remove the leftover particulate matter. A UV–Vis Spectrophotometer (Perkin Elmer-Lambda 25, USA) was used to measure the absorbance of the filtrate at 566 nm. Controls were maintained by using the adsorbent in distilled water and an adsorbent-free AB113. The adsorbed amount of AB113 at equilibrium, q_e (mg/g) was calculated by using Eq. (1).

$$q_e = \left(C_0 - C_e\right)\frac{V}{W} \tag{1}$$

where C_0 and C_e are concentrations (mg/L) of AB113 at initial and equilibrium respectively, V is solution volume (L) and W is adsorbent weight (g).

The same procedure was conducted in kinetic studies also, except the aqueous samples were pre-set at time specific intervals. The concentrations of AB113 were also determined. The amount of AB113 adsorbed at any time, q_t (mg/g), was calculated using Eq. (2).

$$q_t = \left(C_0 - C_t\right)\frac{V}{W} \tag{2}$$

where C_t (mg/L) is the concentration of AB113 measured at time t. Initial concentrations of 50, 100 and 150 mg/L of the dye and an adsorption time of 60 min (5 min intervals) were studied. For determining the optimum amount of adsorbent per unit mass of adsorbate, 50 mL dye solution was brought in contact with varying amounts (0.500–6.000 g/L) of NICSS till equilibrium was attained. To determine the influence of pH on dye adsorption, 50 mg of NICSS along with 50 mL of dye solution of concentration 100 mg/L were agitated on an orbital shaker. The experiment was repeated with varying pH values in range of 2.0–12.0. Equilibrium was reached after 140–150 min with constant agitation speed of 165 rpm. The dye concentration was measured using a double beam UV/Vis spectrophotometer at 590 nm. The pH was adjusted with dilute HCl and/or NaOH. Solution pH was determined by pH meter (Systronics 802, India). The extent of removal of dye was determined by the following equation:

$$\textit{Dye removal efficiency}\ \% = \frac{\left(C_0 - C_e\right)}{C_o} \times 100 \tag{3}$$

All the biosorption experiments were performed in triplicate in the laboratory and results are presented as averages of the replicates.

2.3.1. Adsorption isotherms, adsorption kinetics and thermodynamic parameters

The Langmuir, Freundlich, Jovanovic, Dubinin-Radushkevich, Redlich Peterson, Vieth Sladek, Brouers-Sotolongo, and Sips are the most accepted adsorption isotherm models used for studying the mechanism of equilibrium adsorption for single solute systems at ambient temperature. This analysis helps to describe the interaction between the adsorbate and adsorbent. The results of parameters studied in different models provide information about interaction mechanisms, surface properties and affinities of the adsorbent.

The rate limiting step of the adsorption process was determined by fitting experimental data to the pseudo-first-order and pseudo-second-order kinetic equations.

The effect of diffusion was studied by using the Film Diffusion, Weber–Morris, and Dumwald–Wagner diffusion models. All the models were fitted using the nonlinear least-square method. The controlling mechanism of the adsorption process was found out by fitting the experimental data to the appropriate kinetic equations.

Energy and entropy of a process help understand its feasibility and the mechanism of the adsorption process. In present study, thermodynamic parameters, including standard free energy (ΔG^0), enthalpy change (ΔH^0), and entropy change (ΔS^0) were estimated by using rate law as well as kinetic data to evaluate the extent and enthalpy of the adsorption process.

2.4. Statistical optimization of process parameters

Five factors influencing the adsorption process on the final adsorption capacity were studied and these included: adsorption time (A), process temperature (B), initial dye concentration (C), adsorbent dosage (D) and initial pH (E). These were the independent variables which were to be optimized for adsorption capacity which is the dependent response variable at fixed orbital shaking at 165 rpm. A standard experimental design was prepared comprising 5 factors at 2 levels (Table 1). Analysis of variance was performed on the responses which yielded a general quadratic regression equation. Surface and contour plots were obtained which indicated graphically the effect of individual as well as interaction effects between parameters on the adsorption capacity.

Table 1
Experimental design of high and low levels of factors

Factor	Name	Units	Minimum	Maximum
A	Time	Min	0	180
B	Temperature	°C	27	50
C	Concentration	mg/L	25	500
D	Absorbent dosage	g/L	0.500	6.000
E	pH		2	12

3. Results and discussion

3.1. Characterization of the adsorbent

3.1.1. Surface characterization

NICSS has a visibly fibrous and amorphous morphology because of cellulose and lignocellulose complexes present. The NICSS surface was characterized by SEM which displayed a tortuous porous structure (Fig. 3a). Upon adsorption it is observed that some of the pores are completely filled with the adsorbate (AB113) forming a thin film over the particle (Fig. 3b). The IR spectra of NICSS provide the information of the functional groups present (Fig. 4**)**. The broadband between 3100 and 3500 cm^{-1} in the IR spectrum of NICSS is attributed to the hydroxyl groups of cellulose and adsorbed water molecules. A weak sharp band at 2927 cm^{-1} is due to the C-H stretching and bands at 1743, 1618 and 1514 cm^{-1} is due to C-O stretching. Further, the bands at 1412, 1349, 1260, 1215, 1142 and 1020 cm^{-1} are attributed to the C-O-C stretching. After adsorption of AB113 on NICSS, it has been observed in the IR spectrum that the broad bands

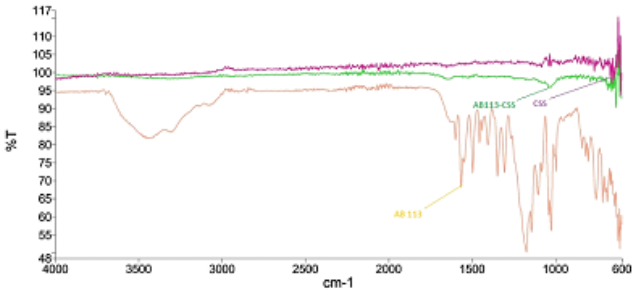

Fig. 4. FTIR spectra of AB113, NICSS and AB113 adsorbed on NICSS.

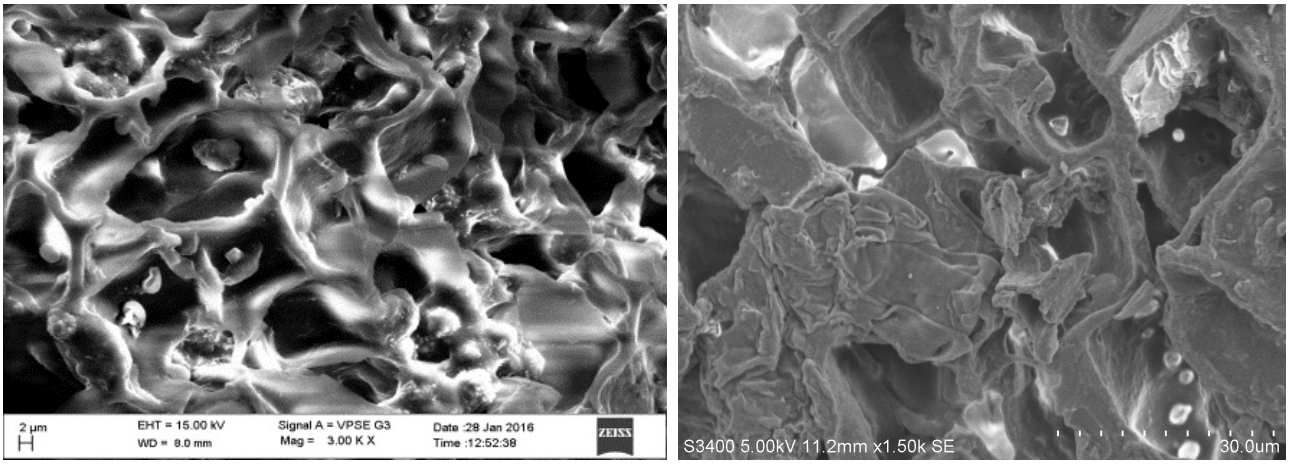

Fig. 3. a) SEM image of NICSS and b) SEM image of AB113-NICSS.

between 3200–3550 cm^{-1} due to N-H stretching of $–NH_2$ group in AB113 and between 3100–3500 cm^{-1} due to the hydroxyl groups of NICSS has disappeared which suggest the possible formation of hydrogen bonds between $–NH_2$ and hydroxyl groups. To confirm the formation of hydrogen bonds the following procedure was adopted. 1 g of NICSS was transferred to a 500-ml Erlenmeyer flask containing 250 ml of 1000 ppm solution. The solution was kept in an incubator at 27 ± 2°C for 24 h with occasional stirring. The solution was filtered through Whatman No 42 filter paper using Buchner funnel apparatus and the AB113 dye adsorbed NICSS was washed with water. The dye adsorbed NICSS was carefully transferred from a Buchner funnel to a watch glass and kept in an oven at 60°C for 24 h for drying. The dried powder was scrapped using spatula and transferred to a bottle. An aliquot amount of the powder was tried for further adsorption as per the procedure detailed in Section 2.3. There was no further adsorption of dye on the already dye-adsorbed NICSS. Thus, the stated reason of possible formation of hydrogen bonds stands augmented and verified. In addition, the disappearance of a strong peak at 1500 cm^{-1} for N-N Stretching in AB113 confirms the strong adsorption of AB113 on NICSS. Finally, based on the disappearance of IR absorption frequencies, it attributes that to a large extent AB113 has adsorbed on NICSS. The point of zero charge for NICSS was found to be pH 7.10 (Fig. 5).

3.2. Batch adsorption studies

3.2.1. Effect of pH and initial dye concentration

It is necessary to determine the optimal parameters for achieving maximum adsorption. The pH is one of the most important parameters for the adsorption process as it controls the adsorption capacity by its influence on the adsorbent surface properties and ionic forms of dye in the solution. The adsorption capacity was the highest when pH was at 2 (Fig. 6a). Adsorption capacity decreased significantly when the pH was increased from 2 to 4 and gradually decreased between pH 4 and 6. Marginal change in the adsorption of the dye was observed between pH 6 and pH 8 and thereafter remained almost constant till pH 12. The higher values of the adsorption capacity of the NICSS at pH 2 is attributed to the formation of OH_2^+ ions on the NICSS surface in the presence of large amounts of H^+ ions. NICSS is a cellulosic material and it is a well-established fact that it contains hydroxyl groups in each separate elementary unit. Decrease in pH results in the increase in the number of OH_2^+ ions on the surface of NICSS. AB113 is a bisazo dye and exhibits anionic charge in solvent of high polarity, such as water. It was found that the maximum AB113 removal by NICSS was maximum at pH 2.0 (q_e = 88 mg/g) with initial concentration of 100 mg/L. Adsorption capacity of 50 mg/g for NICSS was reached for initial AB113 concentration of 100 mg/L (Fig. 6b) at almost neutral pH.

The effect of initial AB113 dye concentration has profound influence on the adsorption capacity of NICSS. The percent adsorption capacity increased with increase in the dye concentration between 25 and 125 mg/L range. The mass transfer phenomena of the dye on to the adsorbent are akin to the increasing driving force generated by the increasing concentration gradient of AB113 dye in the solution phase. This leads to equilibrium adsorption until saturation is attained. Further adsorption of the dye beyond >125 mg/L concentration remains almost similar up till 400 mg/L. At higher initial concentration of the dye (> 400 mg/L) the % q_e decreased with exponential rate (Fig. 6b). This observation is similar to many adsorption studies. Keeping in view the possible commercialization of the experimental data and stringencies pertaining to the E-factor all experiments were carried out below the point of zero charge.

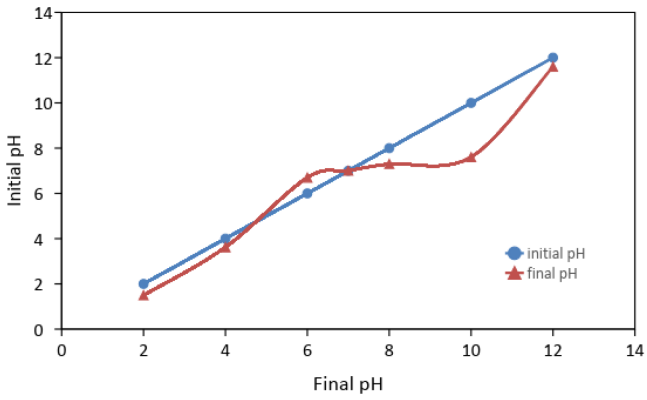

Fig. 5. Point of zero charge of NICSS.

3.2.2. Effect of adsorbent dosage

Adsorbent dose influences the adsorption process, as it decides about extent of adsorption for a given initial concentration of the adsorbate under the operating conditions. The adsorbent dosage of AB113 adsorption was investigated on 0.025–0.300 g in 50 ml of solution. It was observed that the extent of AB113 dye removal from the solution increased with increase in adsorbent dose. Beyond the limit any increase in the adsorbent dose did not result in any change in the amount of adsorption. This is a result of the binding of dye molecules on to the adsorbent surface when equilibrium was reached between dye molecule on the adsorbent and in the solution. The results are depicted in Fig. 6c.

3.2.3. Effect of adsorbent particle size on dye adsorption

Maximum adsorption capacity was studied for initial AB113 concentration of 100 mg/L at neutral pH. The experiments were performed at different particle size of ≤ 90 μm; ≥ 90 μm ≤ 125 μm; ≥ 125 μm ≤ 177 μm; ≥177 μm ≤ 355 μm; ≥355 μm ≤ 500 μm and ≥ 500 μm ≤ 710 μm. The adsorption of dye decreased with the increase in the size of the adsorbent particle (Fig. 6d). The observation is in conformity with the expected results as surface area always decreases when there is increase in adsorbent particle size. An optimum size of ≥ 125 μm ≤ 177 μm (80 mesh ASTM) was selected for the studies because of two reasons: first, 80 mesh particle is widely employed in the fabrication of composites and second, sieving lower size particles will take longer time and adds to the cost of the process.

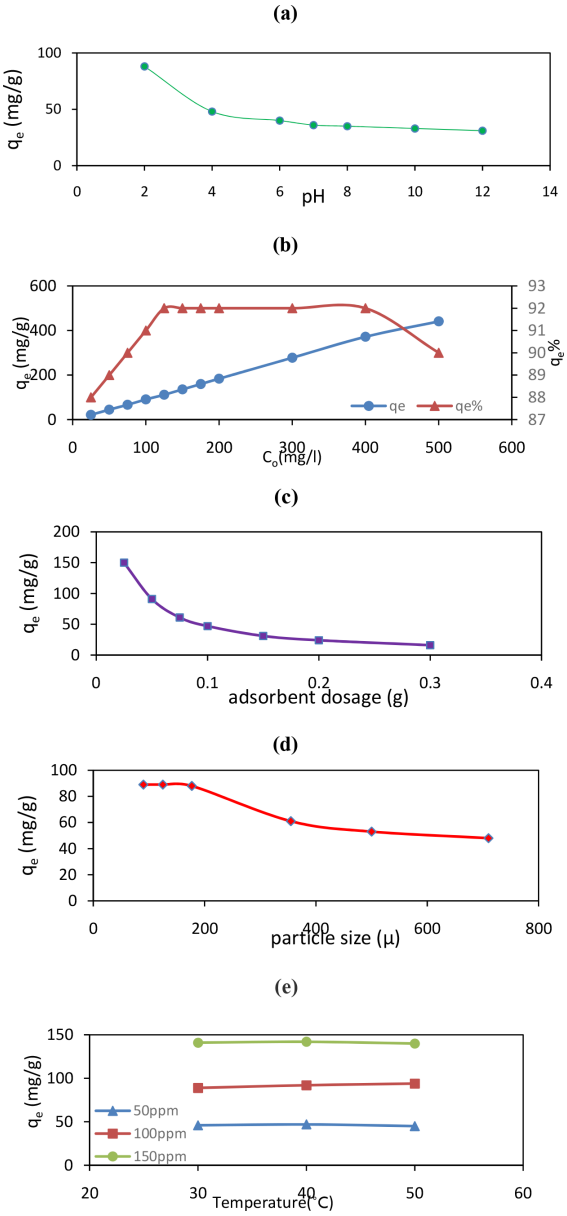

Fig. 6. Effect of a) pH, b) initial dye concentration with percent q_e, c) adsorbent dosage d) particle size and e) temperature.

3.2.4. Effect of temperature

Temperature is an additional factor which influences the adsorption process. The adsorption studies were carried out at 30°C–50°C with three different dye concentrations and the results are shown in Fig. 6e. It can be observed that with increase in temperature, the adsorption capacity decreases gradually, which indicates that the process is endothermic in nature. Increase in adsorption at higher temperature may be a result of higher mobility of dye molecule with decrease in kinetic energy and enhanced rate of intra-particle diffusion [30].

3.2.5. Adsorption isotherm

Adsorption isotherm parameters are important for the description of how molecules of adsorbate interact with adsorbent surface. The Langmuir isotherm model assumes that the mono layer adsorption takes place on to the surface of adsorbent containing finite number of identical adsorption sites of uniform energies [31]. The Langmuir equation is as shown below:

$$q_e = \frac{Q_m K_a C_e}{1 + K_a C_e} R_L = \frac{1}{1 + K_a C_0} \tag{4}$$

where q_e *is* the amount of dye adsorbed on to adsorbent (mg/g) at equilibrium; C_e is the equilibrium concentration (mg/L) of the dye in solution. The values of Q_m and K_a are determined from the intercept and the slope of q_e vs C_e, where, Q_m is the mono layer adsorption capacity (mg/g) and K_a is the Langmuir constant (L/mg) related to the free energy of adsorption. The equilibrium experiments were conducted for different initial concentrations of AB113 in the range of 25–500 mg/L. The Q_m value of 1134.37 mg/g obtained for this isotherm is too high from the experimental value of q_e (90.00 mg/g). However, R^2 value of 0.929 proves that this isotherm has good fit with experimental data.

The separation factor R_L is an important parameter of Langmuir isotherm [32]. The values of R_L describe whether the adsorption in a system studied is unfavourable ($R_L > 1$), Linear ($R_L = 1$), favourable ($0 < R_L < 1$) or irreversible ($R_L = 0$). The R_L values calculated were between 0.86 to 0.24 indicate favourable adsorption of AB113 on to NICSS. The decrease in R_L with an increase in the initial concentration indicates that the adsorption is more favourable at high concentration. However, the large difference between Q_m (1134.37 mg/g) and q_e (90.00 mg/g) has made the authors to explore other adsorption isotherm models.

Freundlich isotherm model is an empirical equation which assumes that the adsorption process takes place on heterogeneous surface [33]. The capacity of adsorption by NICSS is related to the AB113 concentration at equilibrium which follows the equation:

$$q_e = K_F C_e^{1/n_F} \tag{5}$$

where K_F and n_F are the Freundlich constants related to adsorption capacity and adsorption intensity respectively [mg/g and $(mg/L)^{-1/n}$]. The latter is also known as the heterogeneity factor (n_F) which indicates whether the nature of adsorption is linear ($n_F = 1$), chemisorption ($n_F < 1$), or a physisorption ($n_F > 1$). In the present study, the values of n_F = 1.278 and $1/n_F$ = 0.782, indicate that the adsorption is physisorption and favours normal Langmuir Isotherm. The values of K_F and n_F are calculated from the intercept and slope of the plot ln q_e vs. ln C_e. The fitting of Freundlich isotherm to the experimental data has R^2 value of 0.897, where R is the correlation coefficient shows that the process is linear. It could be inferred that the adsorption of AB113 on to NICSS is favourable at experimental conditions and the process is physisorption. Since, no concrete inference was derived from Langmuir and Freundlich models regarding the system being homogenous or heterogeneous, authors have attempted to explore higher models to fit in the data.

Jovanovic isotherm [34] is one of the expanded forms of Langmuir isotherm model. The equation for Jovanovic model is given below:

$$q_e = Q_m\left(1 - e^{(K_j C_e)}\right) \tag{6}$$

where K_j is the Jovanovic constant, q_e is the amount of dye adsorbed on to adsorbent (mg/g) at equilibrium; C_e is the equilibrium concentration (mg/L) of the dye in solution. The model describes formation of a mono layer with no lateral interactions. The added exponential term K_j accounts for deviances of the experimental results from the Langmuir isotherm. The Q_m value of 671.03 mg/g derived from Jovanovich isotherm is high to the experimental value of q_e = 90.00 mg/g. Thus, Jovanovich model fits closer to the experimental q_e value as compared to Langmuir isotherm.

Dubinin-Radushkevich [35] isotherm is another empirical model which initially formulated for the adsorption process following a pore filling mechanism. The equation for Dubinin-Radushkevich isotherm is illustrated below:

$$q_e = q_s\left[\exp\left(-K_{ad}\varepsilon^2\right)\right], Where\ \varepsilon = RT\ln\left[1 + \frac{1}{C_e}\right] \tag{7}$$

where q_s (mg/g) is a constant in the Dubinin-Radushkevich isotherm model which are related to adsorption capacity q_e (mg/g), K_{ad} (mol^2/kJ^2) is a constant in related to the mean free energy of adsorption, R (J/mol/K), and T (K) is the absolute temperature. The Q_m value of 469.12 mg/g which is derived from Dubinin-Radushkevich isotherm is higher than experimental value (q_e = 90.00 mg/g). The fitting of Dubinin-Radushkevich isotherm to the experimental data has R^2 value of 0.968, where R is the correlation coefficient shows that the process is linear. The similarity in χ^2 and R^2 values with Dubinin-Radushkevich model makes it a slightly better fit model when compared to the Langmuir model (Fig. 7).

In brief, the four complimentary two-parameter models studied, suggest that the interaction of AB113 on NICSS is linear, favourable and physical in nature (Tables 2a and 2b). For academic curiosity four three-parameter isotherm models, namely Redlich-Peterson, Brouers-Sotolongo, Vieth-Sladek and Sips were also studied.

The Redlich–Peterson isotherm model [36] was developed to improve the fitting of the Langmuir-Freundlich equations with a correction exponent '*g*'. The equation represents either Langmuir isotherm (*g = 1*) or Freundlich isotherm (*g = 0*). The '*g*' value = 3.434 obtained indicates that the adsorption tends towards Langmuir isotherm. The equation of Redlich-Peterson isotherm is given as:

$$q_e = \frac{A_{RP}C_e}{1 + B_{RP}C_e^g} \tag{8}$$

where A_{RP}, B_{RP} and g are Redlich-Peterson constants, q_e is the amount of dye adsorbed on to adsorbent (mg/g) at equilibrium; C_e is the equilibrium concentration (mg/L) of the dye in solution.

Brouers-Sotolongo isotherm [37] is the mathematical equation consists of K_{BS} and α variables that characterize the adsorption power and the active site distribution of the adsorbent–adsorbate system. Its equation is presented below:

$$q_e = Q_m\left[\left(1 - \exp(-K_{BS}(C_e)^{\alpha}\right)\right] \tag{9}$$

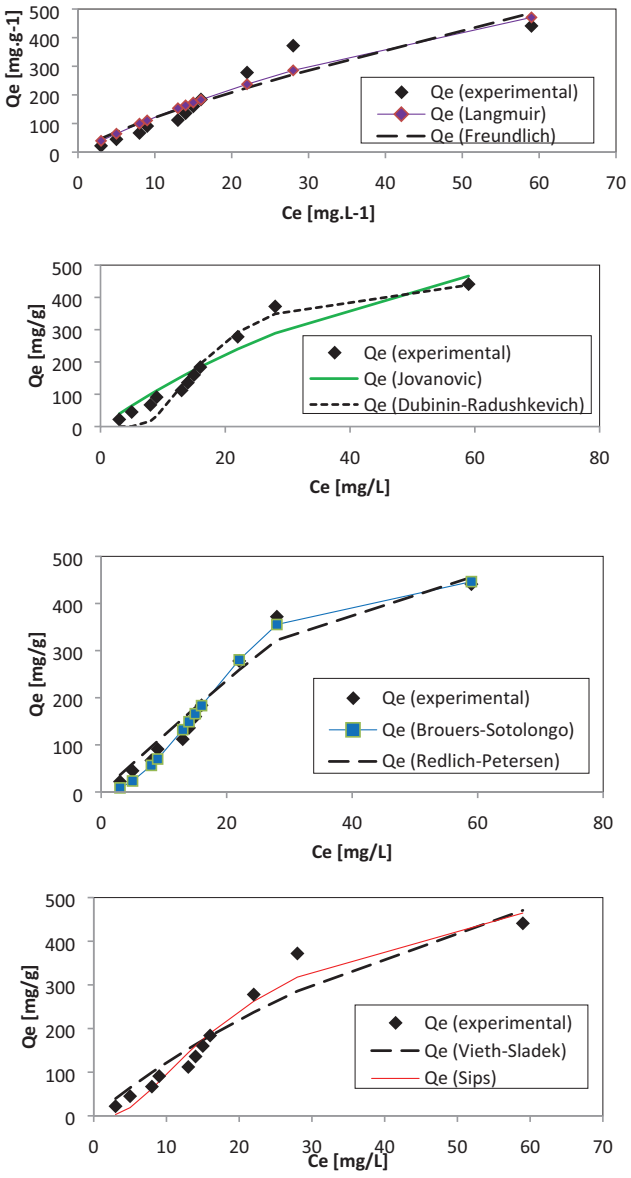

Fig. 7. Fitting of adsorption data to Langmuir, Freundlich, Jovanovic, Dubinin-Radushkevich, Brouers-Sotolongo, Redlich-Petersen, Vieth-Sladek and Sips adsorption isotherm.

where K_{BS} and α are Brouers-Sotolongo constants, q_e is the amount of dye adsorbed on adsorbent (mg/g) at equilibrium, Q_m is the maximum adsorption capacity and C_e is the equilibrium concentration (mg/L) of the dye in solution. The Q_m value of 446.85 mg/g obtained for this isotherm is also high from the experimental value of Q_m (90.00 mg/g). However, the R^2 value of 0.990 shows a good prediction of this isotherm model to the experimental data in Fig. 7.

The Vieth-Sladek isotherm [38] deals with adherence of the dye molecules onto the surface of the adsorbent. The equation of the isotherm is as follows:

$$q_e = K_{VS}C_e + \frac{Qm\beta_{VS}C_e}{1 + \beta_{VS}C_e} \tag{10}$$

where K_{VS} and β_{VS} are Vieth-Sladek constants, q_e is the amount of dye adsorbed on to the adsorbent (mg/g) at equilibrium, Q_m is the maximum adsorption capacity and C_e is the equilibrium concentration (mg/L) of the dye in solution which has value of SSE (14758.2), χ^2 (92.19) and higher value of R^2 (0.929) which makes it a good fit to the experimental values. This model predicts Q_m value of 1134.36 mg/g which is a prediction compared to the Langmuir model studied. In brief, Vieth–Sladek isotherm model is used for estimating diffusion rates in solid materials from transient adsorption.

Sips isotherm [39] has both Langmuir and Freundlich isotherm features. When the adsorbate concentration, is low the Sips equation gets reduced to Freundlich equation. In contrast at high adsorbate concentration, the equation has provision for monolayer adsorption capacity which is equivalent of Langmuir isotherm. The value of Q_m = 661.73 mg/g obtained for Sips isotherm has lesser deviation from experimental value when compared to the value obtained for Langmuir isotherm. Similar lower value of SSE (6862.4), χ^2 (59.07) and higher values of R^2 (0.964) like Langmuir model makes it reasonably good fit with the experimental values. For the most appropriate fitting of the isotherm model and to establish good balance of prediction of Q_m the value should be closer to experimental value. Lower value of χ^2 signifies closer similarity with the experimental data shown in Fig. 7.

In summary, the models used to understand the mechanism of adsorption are of higher order equations. The validity of data fitting cannot be confirmed only by R^2 value because it is used with linear models only. Hence χ^2 values are considered as they provide a better statistic because if model data are similar to the experimental data, then χ^2 would be a small number and vice versa. All the eight isotherm models, gave values for the important parameters (Q_m, χ^2 and R^2) which are shown in Table 2c. Disparity in the values obtained for the parameters of all models studied along with experimental values (q_e) will be of some interest to the scientific community; especially to the mathematical modelling researchers to develop new model that can help for better understanding of the adsorption phenomenon occurring in dye-NIS system.

Table 2a
Calculated parameters of two-parameter isotherms

Two parameter isotherms							
Langmuir		Freundlich		Jovanovic		Dubinin-Radushkevich	
Q_m	1134.37	K_F	20.02	Q_m	671.03	Q_s	469.12
K_S	0.012	n_F	1.278	K_J	2.01E-02	K_{ad}	3.78E-05

Table 2b
Calculated parameters of three-parameter isotherms

Three parameter isotherms							
Redlich-Peterson		Vieth-Sladek		Brouers-Sotolongo		Sips	
A_{RP}	12	Q_m	1134.36	Q_m	446.85	Q_m	661.73
B_{RP}	4.6E-07	K_{VS}	0.0001	K_{BS}	0.0023	K_S	0.49
g	3.434	β_{VS}	0.012	α	1.967	M_S	10.342

3.2.6. Adsorption kinetics

Kinetic models were studied in order to find out the potential rate-controlling steps involved in the process of adsorption. The concentrations of AB113 were 50, 100 and 150 ppm at the time of kinetic studies. Kinetics studies at different temperatures (303 K, 313 K and 323 K) reveal the change in rate of adsorption at different temperature. The adsorption kinetic data were analysed by non-linear analyses (MS Excel 2010) using such kinetic models as: pseudo-first order [40], pseudo-second order [41], intra particle diffusion by Weber-Morris model [42], Dumwald-Wagner model [43] and Film Diffusion model [44]. The estimated parameters are shown in Table 3.

Based on coefficients of determination (R^2) and chi-square values (χ^2) the pseudo-second order model fitted better than pseudo-first order with the experimental data at all initial AB113 concentrations (50, 100 and 150 ppm) at different temperature (Fig. 8). The rate of adsorption was very high initially and slowed down gradually to become stagnant when it reached the maximum adsorption. The adsorption capacity (q_e) increased with increase in temperature. These results show that the adsorption processes were not rate-limiting. The data also show that adsorption process occurred in multiple steps where the solute molecules move from the bulk solution to solid surface followed by diffusion of the solute molecules to the pores of the NICSS.

The Dumwald-Wagner model (Fig. 9) calculates the true absorption rate constant (K) with corrections for observed diffusion effects (Table 4). The Weber-Morris model (Fig. 9) defines that solute uptake varies with $t^{½}$ rather than time of contact (t). Therefore a plot of q_t vs. $t^{½}$ should yield a straight line passing through origin whose slope (k_{int}) is the diffusion rate constant. Adsorption kinetics is not always controlled by single mechanism. It is evident from our experimental data that at all solute concentrations there is multiple levels of linearity. At lower initial concentration (50 ppm) and

Table 2c
Statistical parameters for isotherm model fitting

Isotherms	Langmuir	Freundlich	Jovanovic	Dubinin-Radushkevich	Redlich-Peterson	Vieth-Sladek	Brouers-Sotolongo	Sips
SSE	14758.2	19894.7	13963.99	9777.2	7882.7	14758.2	2130.8	6862.4
R2	0.929	0.897	0.936	0.968	0.972	0.929	0.990	0.964
χ2	92.19	124.76	90.87	148.41	64.65	92.19	31.02	59.07

Table 3
Experimentally determined and theoretically predicted parameters for absorption kinetics models

Initial concentration	Temp		Pseudo first order				Pseudo second order			
[ppm]	[K]	Q_{eexpt} [mg/g]	Q_{epred} [mg/g]	k_1	R^2	χ^2	Q_{epred} [mg/g]	k^2	R^2	χ^2
50	303	46	34.27	2.13E-01	0.58	2.19	37.35	9.00E-03	0.85	0.77
	313	47	35.00	2.11E-01	0.74	1.25	37.34	1.03E-02	0.93	0.31
	323	45	37.53	1.72E-01	0.66	3.25	42.05	5.96E-03	0.87	1.20
100	303	89	61.01	2.30E-01	0.43	5.47	66.67	5.15E-03	0.73	2.52
	313	92	65.87	1.29E-01	0.58	10.14	74.57	2.45E-03	0.76	5.13
	323	94	72.64	1.01E-01	0.67	12.23	83.40	1.69E-03	0.78	6.47
150	303	141	100.61	1.08E-01	0.65	16.51	115.07	1.31E-03	0.78	8.58
	313	142	112.02	7.99E-02	0.76	19.21	131.29	7.96E-04	0.82	10.80
	323	140	117.25	7.61E-02	0.79	18.84	138.49	6.99E-04	0.85	10.52

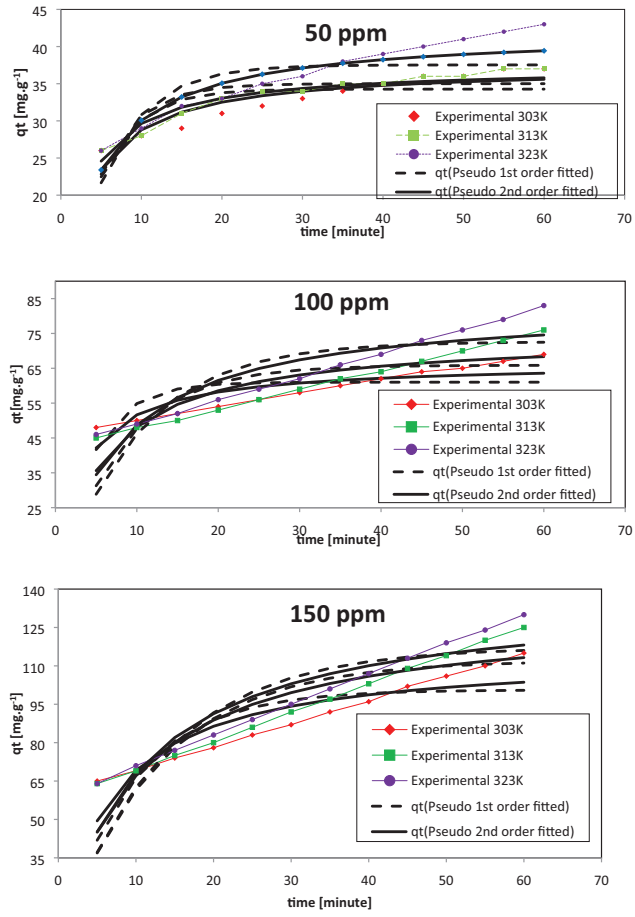

Fig. 8. Kinetic model fits for 50, 100 and 150 ppm initial concentration of AB113 dye on NICSS system at different temperatures.

at lower temperature, the adsorption rate is high and then there is a shift in the rate following a different linear trajectory and finally the rate stabilizes with respect to time. But at higher temperatures the rate is more linear. At higher concentration of solute (150 ppm) there is less apparent changes in the adsorption rate. This is more so when higher temperature data is fitted to the film diffusion model [44]. It is inferred from Fig. 9 that the data shows good adherence to the model with high R^2 and χ^2 values and gives the liquid film diffusion constant R^1 (Table 4). This implies that at higher temperatures the rate of adsorption got hindered negligibly by diffusional limitations. It can be inferred that diffusion is a rate limiting process. The solute initially absorbs quickly onto the surface of the particles forming a film which then gets retarded further, due to diffusion and this explains the changes in absorption rates.

3.2.7. Adsorption thermodynamics

Energy and entropy are the main factors under consideration in the interaction process design. Gibbs free energy change (ΔG°) indicates the extent of spontaneity of adsorption. When the free energy change (ΔG°) of adsorption is negative, significant adsorption occurs. Changes pertaining to Gibbs free energy, entropy and enthalpy of adsorption could be found out by Vant Hoff and Gibbs-Helmholtz equations:

$$K_L = \frac{C_{ac}}{C_e} \tag{11}$$

$$\Delta G° = -RT \ln \ln K_L \tag{12}$$

$$\ln K_L = \frac{\Delta S°}{R} - \frac{\Delta H°}{RT} \tag{13}$$

where K_L is the thermodynamic equilibrium constant (l/mol) and T is the temperature (K). C_{ac} and C_e are the initial and equilibrium concentration (mg/l) of dye in solution respectively. ΔH° and ΔS° can be determined from the slope and the intercept of the Van't Hoff plots of ln (K_L) vs. 1/T and E_a can be determined from the slope and the intercept of the Van't Hoff plots of ln (K_2) vs. 1/T as shown in Figs. 10a and 10b.

The thermodynamic parameter estimates are provided in Table 5. The positive ΔH° value suggests the endothermic nature of adsorption and the negative ΔG° values indicate the feasibility and spontaneity of the adsorption process. The ΔG° is negative for all studied temperatures indicating that the adsorption of AB113 onto NICSS would follow a spontaneous and favorable trend. The ΔG° value decreases with

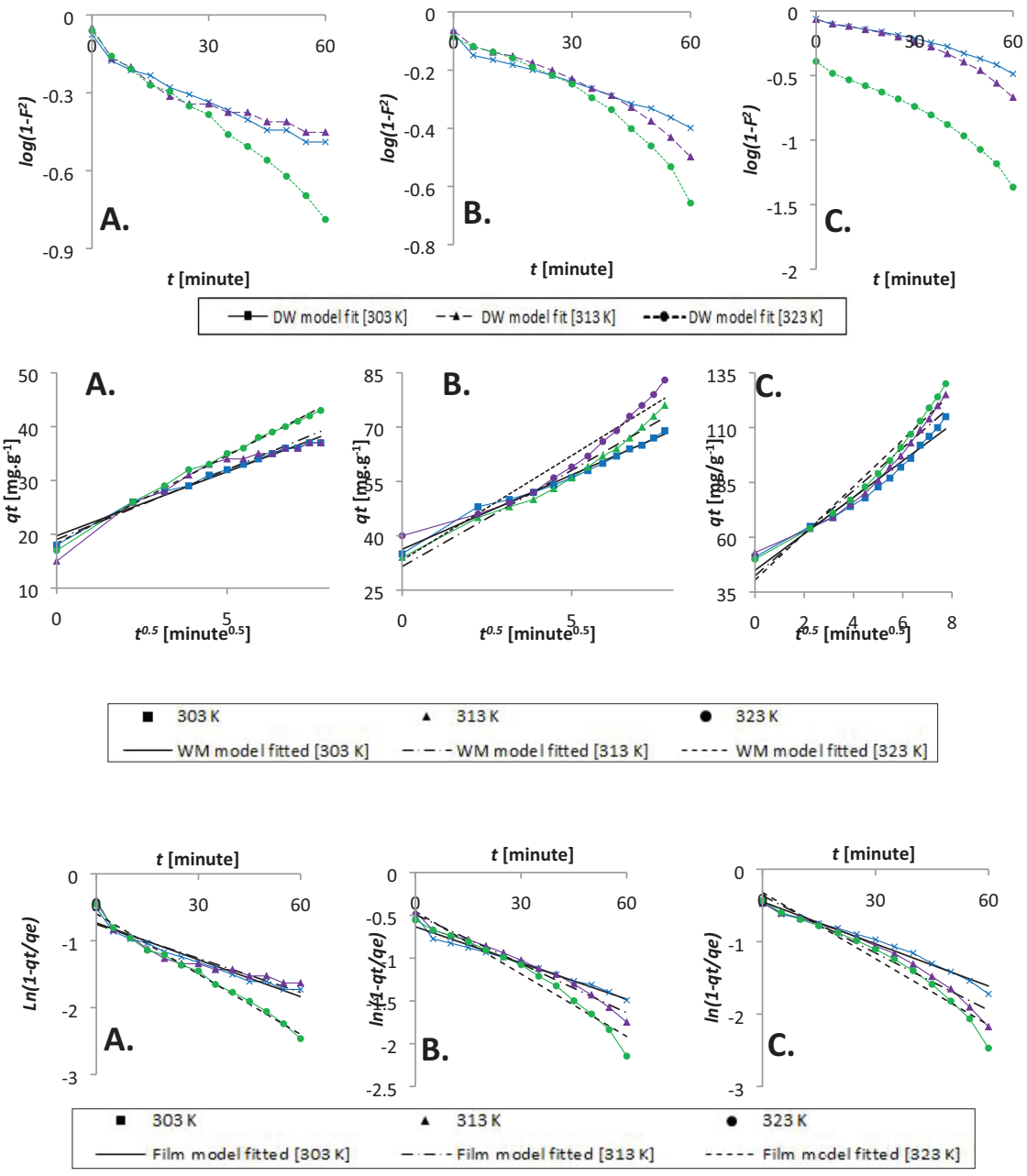

Fig. 9. Kinetics data fitted to the Dumwald-Wagner model, Webber-Morris model and Film diffusion model with initial concentration of AB113 dye a) 50 ppm, b) 100 ppm and c) 150 ppm.

increase in temperature indicating an increase in adsorption at higher temperatures. The positive value of ΔS° suggests good affinity of AB113 towards the adsorbent and increased randomness at the solid solution surface. The extremely low values of ΔH° suggests that the adsorption process is physical as the standard enthalpy change for chemical reaction is normally >200 kJ/mol. This has been further confirmed by activation energy values of the adsorption process at different initial concentrations (50, 100 and 150 ppm) which ranged from ~ –45.48 to –16.47 kJ/ mol using the Arrhenius equation and the kinetic constant from the pseudo-second order model (Table 5).

3.2.8. Statistical optimization by fractional factorial experimental design

The first step in optimization was to determine and fit an appropriate model regression to the experimental data obtained based on fractional factorial experimental design (FFED). The regression equation obtained from the study is shown below:

$$\text{Biosorption} = 78.65 + 44.99*A + 23.90*B + 120.11*C - 85.37*D - 14.69*E - 7.70*AB - 62.22*A^2 + 4.28*B^2 - 76.51*C^2 + 47.85*D^2 - 0.51E^2 \quad (14)$$

Table 4
Calculated parameters for diffusion models

Initial concentration [ppm]	Temp [K]	Film diffusion model		Weber-Morris model		Dumwald-Wagner	
		R| [min^{-1}]	R^2	k_{ist}[mg g^{-1} s$^{-0.5}$]	R^2	K [min^{-1}]	R^2
50	303	0.018	0.95	2.38	0.98	0.015	0.97
	313	0.017	0.84	2.59	0.91	0.013	0.89
	323	0.030	0.99	3.26	0.99	0.026	0.99
100	303	0.014	0.97	4.11	0.99	0.011	0.98
	313	0.019	0.98	5.31	0.98	0.015	0.97
	323	0.024	0.97	5.77	0.94	0.020	0.94
150	303	0.019	0.98	10.66	0.96	0.015	0.96
	313	0.026	0.96	9.72	0.95	0.021	0.93
	323	0.031	0.95	8.32	0.97	0.034	0.96

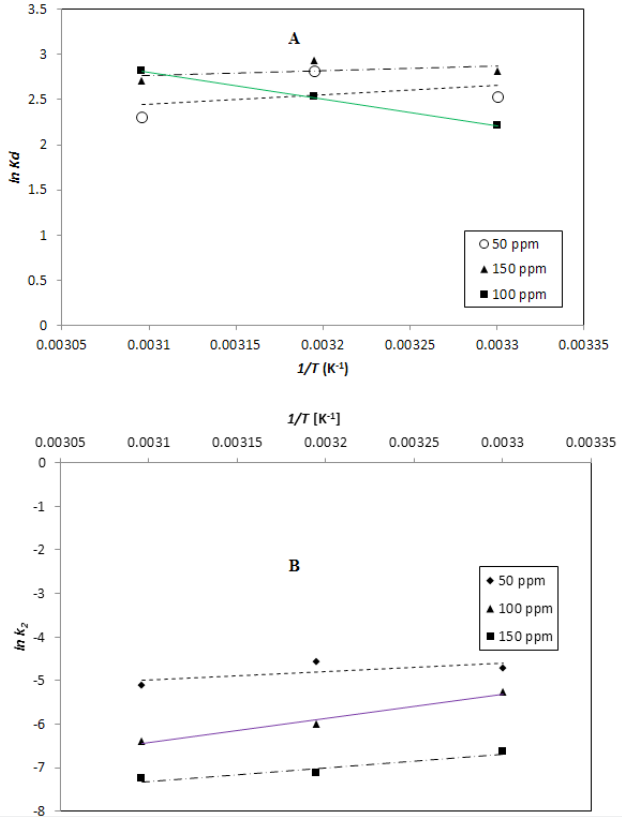

Fig. 10. a) Plot of thermodynamic equilibrium constant vs 1/T to determine the enthalpy and Gibbs free energy of the process and b) Plot of pseudo-second order kinetic constant vs 1/T to determine the activation energy of the process.

Cross product of factors like AD, AE etc. are zero hence excluded from the equation. The optimized values of variables determined by maximizing the second-order polynomial equation using interaction products obtained by multiple regression analysis is as per FFED. Maximum adsorption obtained by the statistical optimization experiment was 226.18 mg/g with optimized conditions established as a pH 2, adsorbent dosage of 0.500 g/L, and an initial dye concentration of 199.47 mg/L for an adsorption time of 121.62 min with orbital shaking of 165 rpm at temperature 49.91°C.

Experiments were carried out with different combinations of five independent variables to study the individual as well as combined effects. The comparison graph for actual vs. predicted values (Fig. 11a) indicates a strong relationship between the experimental and predicted responses. Analysis of Variance (Table 6) obtained from the quadratic regression analysis clearly shows the significance of individual and combined effect of these factors. Significance of factors were considered at confidence interval of 95% with p-value < 0.05%. In this study A, B, C, D, AB, A^2 and C^2 and are significant model terms, E is moderately significant and rest of the variables are insignificant. The derived statistical model seems to be relevant as per the adjusted R^2 value of 84.8%. This high R^2 value and coefficient of variance of 16.60% signify that the model suitably fits the experimentally determined data. As the values of process time and initial dye concentration increase there is an observable increase in adsorption capacity (Fig. 11b, 11c and 11d), whereas, when considering their combined effect there is almost negligible effect. Hence, none of the contour plots and 3D diagrams is included in the text. The values of the regression coefficients, as seen in equation, indicate the effect the parameter has on the adsorption capacity. Positive values indicate incremental effect, for example, an increase in the adsorption time causes a significant increase in adsorption capacity.

Furthermore, the 3D response surface plots and contour plots as function of two independent variables provided the interaction effects between two parameters keeping others at a fixed value. Process optimization statistically in a given range of parameter values, allows not only for calculating the optimal condition, and determines the effect of process conditions on adsorption. The 3D graphs plotted for adsorption time against all other factors indicates that it has a positive effect on the adsorption capacity. By increasing time along with particle size and dye concentration, it is possible to improve the absorption capacity. The absorption maximum is achieved at an absorption time of 121.62 min. The quadratic model developed for process optimization is found to be beneficial for predicting the maximum adsorption capacity and understanding the interaction between independent variables as well as their effect on adsorption

Table 5
Thermodynamic parameters of AB 113-NICSS system

Initial Concentration [ppm]	Temperature [K]	ΔG° [kJ/mol]	ΔS° [J/mol/K]	ΔH° [kJ/mol]	ln A	E_a [kJ/mol]
50	303	–6.36	6.73	8.73	–11.13	–16.47
	313	–7.32				
	323	–6.18				
100	303	–5.56	99.77	24.67	–23.38	–45.48
	313	–6.57				
	323	–7.50				
150	303	–7.09	10.20	4.14	–16.89	–25.71
	313	–7.63				
	323	–7.27				

process. These results indicate that NICSS can be effectively used as an adsorbent for remediation of AB113 from the environment. The adsorption process seems to be thermodynamically feasible and is mainly physical in nature. Furthermore, understanding the kinetics and using FFED we have optimized the process from the perspective of the factors which significantly affect the process, paving the way for scaling it up.

3.2.9. Adsorption mechanism

In the present study, NICSS, the adsorbate, is a cellulosic material comprises of cellulose, hemicellulose and lignin and contains hydroxyl groups in each separate elementary unit. The progression of adsorption is a multi-step activity and is dependent on many factors, such as initial concentration of the dye, particle size of the adsorbent, time of contact between the adsorbent and the adsorbate and pH of the solution. The forces of interaction between adsorbent and the adsorbate include electrostatic forces of attraction, stearic effect, Vander Waals forces and hydrogen bonding. Thus, to elucidate the adsorption mechanism is a major challenge.

AB113 is a sodium salt of bisazo dye which contains two each of azo and sulphonic acid groups and one each of amino and hydroxyl group. The dye ionizes in aqueous solutions to give anionic species as follows: where R denotes the rest of the dye molecule.

$$R–(SO_3)_2\,Na_2 \leftrightarrow R–(SO_3)^{2-} + 2Na^+$$

At lower pH the adsorbent gets protonated which is depicted as follows: Where S stands for adsorbent (NICSS)

$$S–OH + H^+ \leftrightarrow S–OH_2^+$$

The adsorption capacity of AB113 was maximum at pH 2 and decreases with increase in the pH of the solution. The rate of adsorption was very high initially and slowed down gradually to become almost stagnant. Further the FT-IR spectral analysis demonstrates the involvement of –OH, and NH_2 functional groups in the dye adsorption process. In brief, the process of adsorption of the dye onto the adsorbent is governed by mass transfer phenomena. According to the experimental findings and statistical optimization of process parameters the mechanism of adsorption involves the following steps:

- Mass transfer of AB113 dye from bulk solution onto the adsorbent is fast at the initial stages till monolayer is formed.
- Mechanical agitation has profound influence on mass transfer.
- Diffusion is a slow process.
- The hydrogen bonds are formed between –OH groups of NICSS and $–NH_2$ group of AB113
- The influence of weak Vander Waals forces plays a major role.
- Electrostatic forces of attraction between the anionic dye and $–OH_2^+$ group of NICSS.

On the basis of the above physical model of the interaction of adsorbent and adsorbate is drawn and shown in Fig. 12.

4. Application of proposed method to textile industrial effluent

Different processes employed in textile industry generate waste water with varied composition containing, large amounts of suspended solids, highly fluctuating pH, variable temperature, intense color and COD concentration [45]. Therefore, it is difficult to identify a specific dye in industrial effluent due to matrix effect [46]. A simple procedure was developed to compare the remediation of AB113 dye in water as also in textile industrial effluent.

4.1. Textile industrial effluent (TIE)

Effluent samples were collected from a local textile industry which operates in two shifts. Six random TIE samples were collected in 10-L polyethylene containers from the end of the pipe where the effluent enters into the treat-

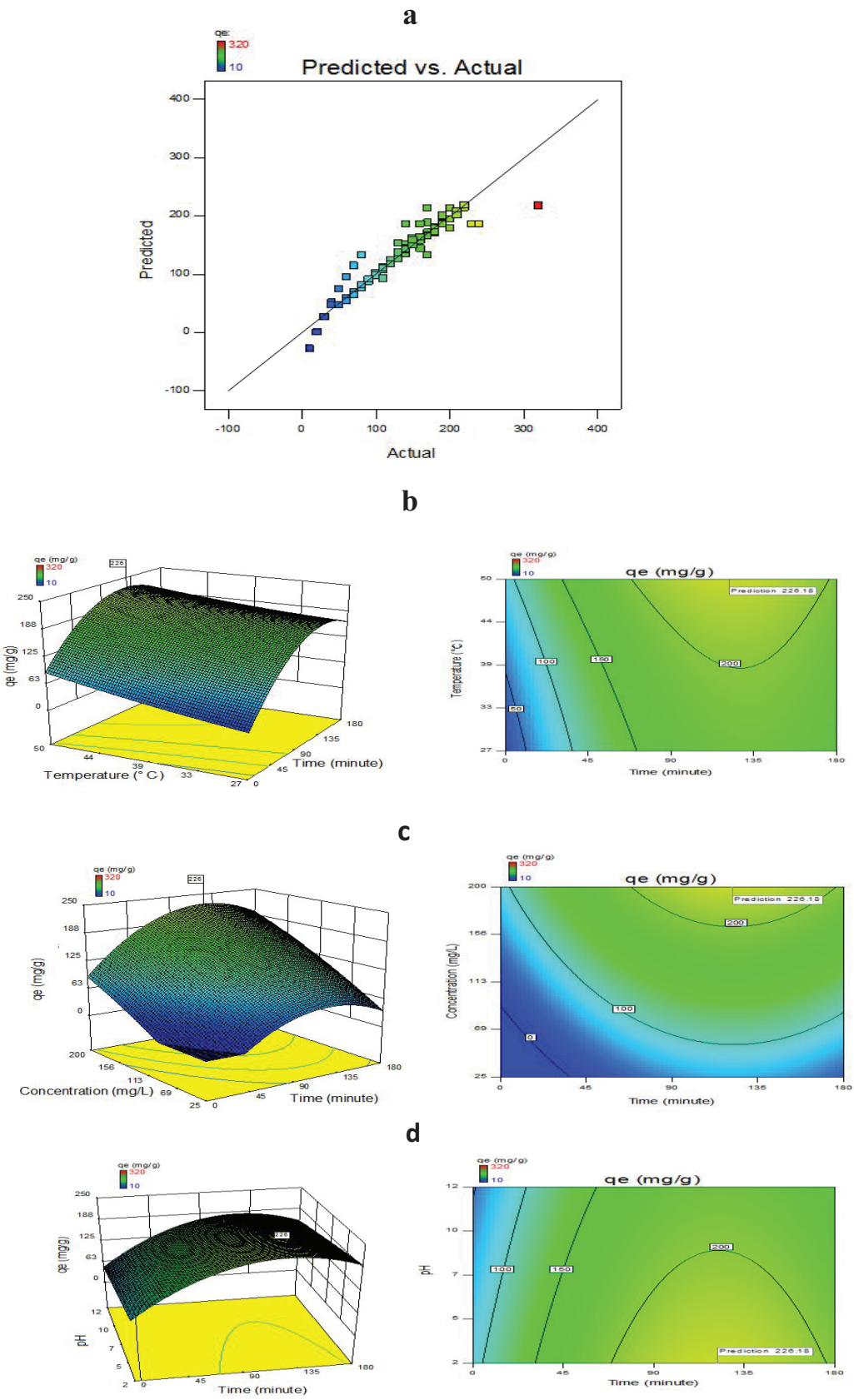

Fig. 11. a) Comparison graph for actual versus predicted values, 3D surface plot and contour plot showing the variation of adsorption capacity with b) time versus temperature, c) time versus concentration and d) time versus pH.

Table 6
ANOVA for fractional factorial experimental design

Source	Sum of Squares	Degree of freedom	Mean Square	F Value	P- Value
Model	220975.8	11	20088.71	41.21637	< 0.0001**
A	55471.19	1	55471.19	113.8112	< 0.0001**
B	13161.15	1	13161.15	27.00296	< 0.0001**
C	56328.68	1	56328.68	115.5706	< 0.0001**
D	28273.67	1	28273.67	58.00961	< 0.0001**
E	2039.714	1	2039.714	4.184919	0.045*
AB	842.6007	1	842.6007	1.728779	0.192984
A^2	29561.57	1	29561.57	60.65201	< 0.0001**
B^2	171.7577	1	171.7577	0.352398	0.56
C^2	10538.06	1	10538.06	21.62113	< 0.0001**
D^2	2492.399	1	2492.399	5.1137	0.03*
E^2	1.863012	1	1.863012	0.003822	0.95
Residual	33142.95	68	487.3964		
Lack of fit	25667.95	65	394.8916	0.158485	0.9992
Total	254118.8	79			

Significant figures
+Suggestive significance (p value: 0.05 < p < 0.10)
*Moderately significant (p value: 0.01 < p < 0.05)
**Strongly significant (p value: p < 0.01)

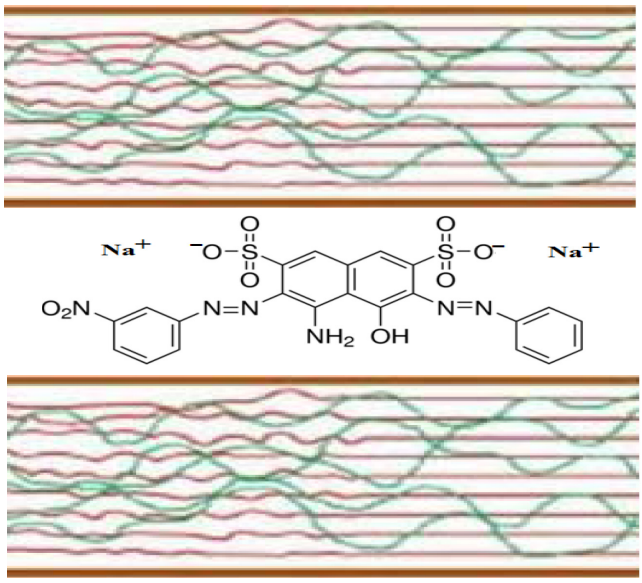

Fig. 12. Plausible mechanism of interaction of NICSS with AB113 dye.

ment plant. Among the six samples, three were collected from first and second shifts consecutively on three working days. All textile industrial effluent samples collected were transferred to a 100-L barrel and stirred manually to get uniform concentration. The resulting TIE solution was used as control sample for analyses. Sampling, preparation and preservation methods followed while collecting the effluent samples from the industries were in accordance with standard methods [47].

4.2. Preparation of AB113 in distilled water

2 g of AB113 were transferred to a 2-L standard flask. The dye was dissolved in distilled water and the solution was made up to the mark. The resulting solution was stirred to uniform concentration (Solution 1).

4.3. Preparation of AB113 in textile industrial effluent

2 g of AB113 were transferred to a 2-L standard flask. The dye was dissolved in TIE and the solution was made up to the mark with TIE. The resulting solution was stirred to uniform concentration (Solution 2).

4.4. Blank experiment

Five hundred ml of distilled water were transferred to a one-liter conical flask containing 5-cm Teflon coated magnetic bar. Five grams of NICSS were added and the solution stirred at about 700 rpm for 15 min using a magnetic stirrer. The solution was filtered using No 42 Whatman filter paper and the filtrate solution was compared with the solution obtained after remediation of dye loaded-TIE.

4.5. Procedures

4.5.1. Measurement of the absorbance of stock solutions

An aliquot solution of TIE was filtered through Buchner funnel apparatus using No 42 Whatman filter paper and the absorbance of the filtrate was measured using UV-Vis Spectrophotometer (Perkin Elmer-Lambda 25, USA) with a maximum absorbance scale of 3.0. All the absorbance was measured within this range. However, in case of concen-

trated solutions,the absorbance was measured after appropriate dilution and the resultant absorbance was multiplied by the dilution factor to get the absorbance of concentrated solution. This procedure was repeated to measure the absorbance of Solution 1 and Solution 2.

4.5.2. Measurement of molar absorption coefficient (ε) of AB113

Six different concentrations (0.625×10^{-4}; 1.25×10^{-4}; 2.50×10^{-4}; 5.00×10^{-4}; 7.50×10^{-4} and 10.00×10^{-4}) of AB113 were prepared in distilled water and the absorbance was measured at 566 nm using distilled water as reference (Fig. 13a). A graph of absorbance vs. concentration was plotted. ε was measured from the slope of the linear portion of the curve or by using mathematical formula ε = A/cl where A is specific absorption coefficient for concentration c (mol/L) for a path length of 1 cm. Specific absorption coefficient or absorbency index is the absorbance per unit path length and unit concentration. In case of the latter the εAB113 was calculated as the mean of six values as follows:

$$\varepsilon AB113 = \varepsilon 1 + \varepsilon 2 + \varepsilon 3 + \varepsilon 4 + \varepsilon 5 + \varepsilon 6/6$$

$$\varepsilon AB113 = 2450 + 2440 + 2424 + 2402 + 2396 + 2411/6 = 2421$$

Step 1: Five hundred ml of Solution 1 were transferred to one-liter conical flask. Five gram of NICSS was added to the conical flask and the solution was agitated using magnetic stirrer at about 700 rpm. At the end of 15 min the agitation was stopped and solution was filtered through No 42 Whatman filter paper using Buchner funnel apparatus. If the filtrate is not clear the filtration was repeated and absorbance recorded.

Step 2: The dye-adsorbed NICSS on the filter paper of the Step 1 was carefully transferred from a Buchner funnel to a watch glass and kept in an oven at 60°C for 24 h for drying. The dried powder was scrapped using spatula and transferred to a watch-glass.

Step 3: Second portion of 5 g NICSS added to the conical flask containing filtrate solution from Step 1 and agitation was continued on a magnetic stirrer at about 700 rpm for 15 min. At the end of 15 min the agitation was stopped and solution was filtered through No 42 Whatman filter paper using Buchner funnel apparatus. If the filtrate is not clear the filtration was repeated and absorbance recorded.

Step 4: The dye-adsorbed NICSS on the filter paper of the Step 3 was carefully transferred from a Buchner funnel to a watch glass and kept in an oven at 60°C for 24 h for drying. The dried powder was scrapped using spatula and transferred to a watch-glass.

Step 5: Third portion of 5 g NICSS was added to the conical flask containing filtrate solution from Step 3 and agitation was continued on a magnetic stirrer at about 700 rpm for 15 min. At the end of 15 min the agitation was stopped and solution was filtered through No 42 Whatman filter paper using Buchner funnel apparatus. If the filtrate is not clear the filtration was repeated and absorbance recorded.

Step 6: The dye-adsorbed NICSS on the filter paper of the Step 5 was carefully transferred from a Buchner funnel to a watch glass and kept in an oven at 60°C for 24 h for drying. The dried powder was scrapped using spatula and transferred to a watch-glass.

Step 7: Fourth portion of 5 g NICSS was added to the conical flask containing filtrate solution from Step 5 and agitation was continued on a magnetic stirrer at about 700 rpm for 15 min. At the end of 15 min the agitation was stopped and solution was filtered through No 42 Whatman filter paper using Buchner funnel apparatus. If the filtrate is not clear the filtration was repeated and absorbance recorded.

Step 8: The dye-adsorbed NICSS on the filter paper of the Step 7 was carefully transferred from a Buchner funnel to a watch glass and kept in an oven at 60°C for 24 h for drying. The dried powder was scrapped using spatula and transferred to a watch-glass.

Step 9: Steps 1 to 8 were repeated with Solution 2.

The powder and filtrate solutions after the adsorption of constituents of Solution 2 on NICSS are shown in Figs. 13b and 13c.

Preliminary trial study revealed that better results could be obtained by scaling up to two-orders of the adsorbent and the adsorbate and to one order of the volume of the solution. In an interesting observation Solution 2 showed about 20% decrease in absorbance compared to Solution 1. This may be due to the absorbance of the dye by varied

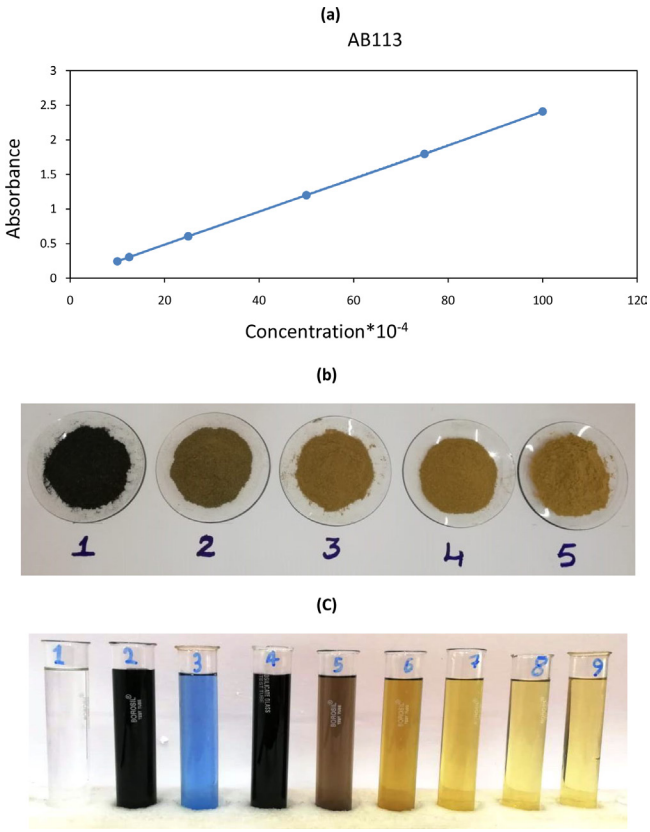

Fig. 13. a) Determination of molecular extinction coefficient of AB113 dye, b) Powders 1 to 4: Fresh samples of NICSS added to AB113-TIE solution after every 15 min, filtered and the residue dried in oven. Sample 5: NICSS and c) Color of the solutions before and after adsorption: 1. Distilled water; 2. AB113 in distilled water; 3. TIE; 4. AB113 in TIE; 5. Filtrate after adsorption of dye on NICSS after 15 min; 6. 30 min; 7. 45 min; 8. 60 min; 9. Filtrate of NICSS in distilled water.

undefined constituents present in TIE. Also, it was observed that additional fresh samples of the adsorbent after every 15 min enhanced the efficiency of removal of the dye from TIE. The recovery of the dye and allied substances from Solution 2 to an extent of 75%, 90%, 93% and 95% after 15, 30, 45 and 60 min respectively was observed. This observation is in accordance with the kinetic results according to which the solute adsorbs quickly onto the surface of the particles forming a film which then gets retarded further diffusion thereby bringing change in absorption rates.

The experiment was scaled up to 10 g, 20 g, and 50 g of NICSS using 1, 2, and 5 L of Solution 2 taken in polyethylene beakers. The solutions were vigorously stirred using a magnetic stirrer and the procedure repeated as indicated earlier and the results obtained were almost uniform. All experiments were carried out in triplicate and the mean of three results are reported. The coefficients of variance of all results did not exceed ± 2% error.

In brief, an attempt to increase the scale of experiment by about three orders of its initial set up has given promising results. The industrial effluents may have many variables that may not be exactly interpreted from the initial data. This is always a serious limitation in such studies. The outcome could be pin pointedly focused by resorting to much larger pilot scale study. However, the fact that the limitations of scale have been recognized, and that the enhanced scale experimental data will definitely continue to show promise and reliability of the process, which fact may be sufficient to prove that the principles of the method when put into development on a larger scale in industries will show its usefulness.

4.5.3. Regeneration of the adsorbent and cost analysis

Regeneration of dye-loaded NICSS enables its re-use and recovery of the adsorbed material. This may not prove economical as the process cost and the cost of solvents will be much more when compared to the cost of the adsorbent (< 1 US$ for 10 Kg NICSS) used in the process. Added to this it will also enhance the E-factor [16] which is undesirable due to unprecedented load of environmental toxicants. The work is in progress in our laboratory to use dye adsorbed nutraceutical industrial spent as filler/reinforcing material and a some interesting results have come out which are published elsewhere [17,26].

5. Conclusion

In order to give value-addition to the spent generated in nutraceutical industries, NICSS has been used as a biosorbent for the remediation of toxic dyes. NICSS proved as effective adsorbent of AB113 from aqueous solution. The AB113 adsorption process is endothermic and almost spontaneous. The results fitted well with pseudo-second-order kinetic model. There was significant effect of film on intra-particular diffusion and the process is predominantly physical. The SEM and FTIR spectra confirmed the adsorption of AB113 onto NICSS. The technology of utilization of spent material from nutraceutical industries is a cleaner, cheaper and efficient way of using the Nutraceutical Industrial Spent as an adsorbent to control pollution.

In summary, the unprecedented rise of nutraceutical industries as a predominant sector of world's economy is generating myriad tons of renewable spent/waste. This is seriously affecting the environment. In such a situation, nutraceutical industrial sector, as a part of agro-industries cannot continue to pollute the environment for a long period. In order to sustain nutraceutical industrial development there is an urgent need for an effective management of nutraceutical spent and/or waste. Reuse, regeneration and recovery are the main aspects of recycling, and these are the curative approaches involved in environmental management. This paper aims in achieving that goal.

Acknowledgments

The author (SNT) gratefully acknowledges University of Malaya for the award of Post Graduate Research Grant (PG 213-2014B) and Fundamental Research Grant Scheme (FRGS-FP052-2016).

Conflict of interest

All authors declare no conflict of interest.

Symbols

C_e — Equilibrium concentration (mg/L)
C_o — Initial concentration (mg/L)
n_F — Heterogeneity factor
q_e — Adsorption capacity (mg/L)
Q_m — Maximum adsorption capacity (mg/g)
q_t — Adsorption capacity at time 't' (mg/L)
R^2 — Correlation coefficient
R_L — Separation factor
SSE — Sum of square errors
ΔG^0 — Standard free energy
ΔH^0 — Enthalpy change
ΔS^0 — Entropy change
χ^2 — Chi-squared test

References

[1] V. Zaffalon, Climate change, carbon mitigation and textiles, Textile World, 160 (2010) 34–35.
[2] C.J. Ogugbue, T. Sawidis, Bioremediation and detoxification of synthetic wastewater containing triarylmethane dyes by aeromonas hydrophila isolated from industrial effluent, Biotech. Res. Int., (2011) 1–11. doi:10.4061/2011/967925.
[3] Z. Yao, L. Wang, J. Qi, Biosorption of methylene blue from aqueous solution using a bioenergy forest waste: Xanthoceras sorbifolia seed coat, CLEAN–Soil. Air Water, 37 (2009) 642–648.
[4] M.A. Hubbe, S.H. Hasan, J.J. Ducoste, Cellulosic substrates for removal of pollutants from aqueous systems: A review. 1. Metals, Bio. Resour., 6 (2011) 2161–2287.
[5] A. Bafana, S.S. Devi, T. Chakrabarti, Azo dyes: past, present and the future, Environ. Rev., 19 (2011) 350–371.
[6] C.M. Carliell, S.J. Barclay, C. Shaw, A.D. Wheatley, C.A. Buckley, The effect of salts used in textile dyeing on microbial decolourisation of a reactive azo dye, Environ. Technol., 19 (2011) 1133–1137.

[7] R.D. Combes, R.B. Haveland-Smith, A review of the genotoxicity of food, drug and cosmetic colours and other azo, triphenylmethane and xanthene dyes, Mutat. Res., 98 (1982) 101–243.
[8] F.J. Green, The sigma-aldrich handbook of stains, dyes and indicators, Aldrich Chemical Co., (1990).
[9] R.O.A. de Lima, A.P. Bazo, D.M.F. Salvadori, C.M. Rech, D. de Palma Oliveira, G. de Aragão Umbuzeiro, Mutagenic and carcinogenic potential of a textile azo dye processing plant effluent that impacts a drinking water source, Mutat. Res., 626 (2007) 53–60.
[10] A. Szyguła, E. Guibal, M. Ruiz, A.M. Sastre, The removal of sulphonated azo-dyes by coagulation with chitosan, Colloids. Surf. A., 330 (2008) 219–226.
[11] M.M. Dávila-Jiménez, M.P. Elizalde-González, A.A. Peláez-Cid, Adsorption interaction between natural adsorbents and textile dyes in aqueous solution, Colloids. Surf A., 254 (2005) 107–114.
[12] M.A. Zazooli, J. Yazdani, D. Balarak, M. Ebrahimi, Y. Mahdavi, Investigating the removal rate of acid blue 113 from aqueous solution by canola, JMUMS., 22 (2013) 71–78.
[13] M.R. Unnithan, T.S. Anirudhan, The kinetics and thermodynamics of sorption of chromium (VI) onto the iron (III) complex of a carboxylated polyacrylamide-grafted sawdust, Ind. Eng. Chem. Res., 40 (2001) 2693–2701.
[14] http://www.mrssindia.com/uploads/reports/pdf/assocham-knowledge-report-on- nutracuticals released-at-3rd-national-symposium-6.pdf (accessed November 28, 2018).
[15] K.V. Peter, (Ed) Handbook of herbs and spices, Wood head publishing, 3 (2006).
[16] R.A. Sheldon, Organic synthesis-past, present and future, Chem. Ind., 23 (1992) 903–906.
[17] S.N. Taqui, R. Yahya, A. Hassan, N. Nayak, A.A. Syed, A novel sustainable design to develop polypropylene and unsaturated polyester resin polymer composites from waste of major polluting industries and investigation on their physicomechanical and wear properties, Polym. Compos., (2018) doi:10.1002/pc.24819.
[18] M.A. Syed, A.A. Syed, Development of green thermoplastic composites from centella spent and study of its physicomechanical, tribological, and morphological characteristics, J. Thermoplast. Compos. Mater., 29 (2016) 1297–1311.
[19] M.A. Syed, A.A. Syed, Investigation on physicomechanical and wear properties of new green thermoplastic composites, Polym. Compos., 37 (2016) 2306–2312.
[20] M.A. Syed, A.A. Syed, Development of a new inexpensive green thermoplastic composite and evaluation of its physico-mechanical and wear properties, Mater. Des., 36 (2012) 421–427.
[21] S. Pashaei, Siddaramaiah, A.A. Syed, Investigation on mechanical, thermal and morphological behaviors of turmeric spent incorporated vinyl ester green composites, Polym. Plast. Technol. Eng., 50 (2011) 1187–1198.
[22] M.A. Syed, S. Akhtar, A.A. Syed, Studies on the physico-mechanical, thermal and morphological behaviors of high density polyethylene/coleus spent green composites, J. Appl. Polym. Sci., 119 (2011) 1889–1895.
[23] M.A. Syed, B. Ramaraj, S. Akhtar, A.A. Syed, Development of environmentally friendly high density polyethylene and turmeric spent composites: Physicomechanical, thermal, and morphological studies, J. Appl. Polym. Sci., 118 (2010) 1204–1210.
[24] M.A. Syed, Siddaramaiah, R.T. Syed, A.A. Syed, Investigation on physico-mechanical properties, water, thermal and chemical ageing of unsaturated polyester/turmeric spent composites, Polym. Plast. Technol. Eng., 49 (2010) 555–559.
[25] M.A. Syed, Siddaramaiah, B. Suresha, A.A. Syed, Mechanical and abrasive wear behavior of coleus spent filled unsaturated polyester/polymethyl methacrylate semi interpenetrating polymer network composites, J. Compos. Mater., 43 (2009) 2387–2400.
[26] S.N. Taqui, R. Yahya, A. Hassan, N. Nayak, A.A. Syed, Development of sustainable dye adsorption system using nutraceutical industrial fennel seed spent—studies using congo red dye, Int. J. Phytoremediation, 19 (2017) 686–694.
[27] P.K. Papegowda, A.A. Syed, Isotherm, kinetic and thermodynamic studies on the removal of methylene blue dye from aqueous solution using saw palmetto spent, Int. J. Environ. Res., 11 (2017) 91–98.
[28] R. Sulthana, S.N. Taqui, F. Zameer, S.U. Taqui, A.A. Syed, Adsorption of ethidium bromide from aqueous solution on to nutraceutical industrial fennel seed spent: Kinetics and thermodynamics modeling Studies, Int. J. Phytoremediation, 20 (2018) 1075–1086.
[29] R. Ahmad, R. Kumar, Adsorption studies of hazardous malachite green onto treated ginger waste, J. Environ. Manage., 91 (2010) 1032–1038.
[30] S. Chowdhury, P. Das, Utilization of a domestic waste—Eggshells for removal of hazardous malachite green from aqueous solutions, Environ. Prog. Sustain. Energy, 31 (2012) 415–425.
[31] I. Langmuir, The constitution and fundamental properties of solids and liquids, J. Am. Chem. Soc., 38 (1916) 2221–2295.
[32] T.W. Webber, R.K. Chakkravorti, Pore and solid diffusion models for fixed-bed adsorbers, Alche. J., 20 (1974) 228–238.
[33] H.M.F. Freundlich, Over the adsorption in solution, J. Phys. Chem., 57 (1906) 385–471.
[34] D.S. Jovanović, Physical adsorption of gases, Colloid. Polym. Sci., 235 (1969) 1203–1213.
[35] M.M. Dubinin, The equation of the characteristic curve of activated charcoal, In Dokl. Akad. Nauk. SSSR., 55 (1947) 327–329.
[36] O.J.D.L. Redlich, D.L. Peterson, A useful adsorption isotherm, J. Phys. Chem., 63 (1959) 1024.
[37] F. Brouers, O. Sotolongo, F. Marquez, J.P Pirard, Microporous and heterogeneous surface adsorption isotherms arising from levy distributions, Physica. A. Stat. Mech. Appli., 349 (2005) 271–282.
[38] W.R. Vieth, K.J. Sladek, A model for diffusion in a glassy polymer, J. Colloid. Sci., 20 (1965) 1014–1033.
[39] R. Sips, Combined form of langmuir and freundlich equations, J. Phys. Chem., 16 (1948) 490–495.
[40] S. Lagergren, About the theory of so-called adsorption of soluble substances, Kungliga. Svenska. Vetenskapsakademiens. Handlingar, 24 (1898) 1–39.
[41] Y.S. Ho, G. McKay, Sorption of dye from aqueous solution by peat, Chem. Eng. J., 70 (1998) 115–124.
[42] M. Alkan, Ö. Demirbaş, M. Doğan, Adsorption kinetics and thermodynamics of an anionic dye onto sepiolite, Microporous. Mesoporous. Mater., 101 (2007) 388–396.
[43] H.L. Wang, J.L. Chen, Z.C. Zhai, Study on thermodynamics and kinetics of adsorption of p-toluidine from aqueous solution by hyper cross linked polymeric adsorbents, Environ. Chem., 23 (2004) 188–192.
[44] G.E. Boyd, A.W. Adamson, L.S. Myers Jr, The exchange adsorption of ions from aqueous solutions by organic zeolites. II. Kinetics, J. Am. Chem. Soc., 69 (1947) 2836–2848.
[45] P. Kumar, B. Prasad, I.M. Mishra, S. Chand, Catalytic thermal treatment of desizing waste waters, J. Hazard. Mater., 149 (2007) 26–34.
[46] A.M. Talarposhti, T. Donnelly, G.K. Anderson, Colour removal from a simulated dye wastewater using a two-phase anaerobic packed bed reactor, Water Res., 35 (2001) 425–432.
[47] Standard methods for the examination of water and wastewater, 20th edn, American Public Health Association, Washington DC, 2002.